

## RESEARCH PAPER

# Structural Response of AISC- composite concrete filled circular steel Columns under Lateral Load

Sinan Abdulkhaleq Yaseen<sup>1</sup>, Muhammed Ali Ihsan Saber<sup>2</sup> and Bayan Salim Al-Numan<sup>3</sup>

<sup>1,2</sup> Department of Civil Engineering, College of Engineering, Salahaddin University-Erbil, Kurdistan Region, Iraq

<sup>3</sup> Civil Engineering Department, Tishk International University

### ABSTRACT:

In this article, there is a theoretical behavior research of composite frames consist of American Institute of Steel Construction (AISC)-composite pipes-filled with concrete to act as circular steel columns joined with steel beams subjected to unchanged axial loads and a lateral increasing load. The effects of column height and skin thickness, based on those available in the AISC manual, on the load-deformation reaction of composite frames, including steel tubes filled with concrete STFC, loaded by maximum vertical load allowed by AISC manual, were studied. A ANSYS program was used to develop a finite element (FE) model. This simulation considers linear and non-linear response of the composite materials. The obtained outcomes from the FE analysis were presented and discussed. Over the range of column heights (from 3048 mm to 6096 mm), no buckling has been reached and failure modes were observed after formation of plastic hinges at the connection of beam-column. For skin thicknesses (from 14.76 mm to 5.92 mm), varied load-deformation responses have been obtained. Stiffer Responses were obtained for skin thickness 14.76 mm. Lateral load range at failure was from 9.2 to 20.8 % of the maximum AISC vertical load, and displacement ductility was ranged from 1.71 to 3.08 for circular-STFC frames.

KEY WORDS: Composite frames; steel tubes filled with concrete; finite element modelling

DOI: <http://dx.doi.org/10.21271/ZJPAS.32.4.4>

ZJPAS (2020) , 32(4);30-37 .

### 1. INTRODUCTION:

Due to high strength, stiffness and ductility of steel tubes filled with concrete STFC, they are used in buildings to carry lateral static/dynamic forces. Many research works were published for the analysis of STFC investigating the most effective parameters on their structural behavior. Shams (Shams & Saadeghvaziri ,1997) published on safety factors for short tubular STFC. Zhao et al (Zhao & Grzebieta, 1999) published a research on SHS filled beams under cyclic loading. Schneider (Schneider, 1998) developed a nonlinear 3D finite element models for STFC elements by ABAQUS program.

Hu et al [Hu et al., 2003) used ABAQUS for circular section, square section, and square section stiffened by reinforcing ties to develop FE nonlinear model to investigate the behavior of STFC. Numerical trial-and-error method was used to capture concrete properties to fit the analysis to experimental results. Han et al (Han et al., 2007) used ABAQUS for modelling STFC that loaded by uniaxial compression for confined core concrete of STFC. Lin-Hai et al (Lin-Hai et al., 2008) used ABAQUS to model STFC framed to steel beams. FE modelling was developed to analyze the frame under cyclic loading. Analysis was verified by 6 tested frames. Lin-Hai et al (Lin-Hai et al.2011) studied on the behavior of composite frames with steel tubes filled with concrete (STFC) columns joined with steel beam under unchanged axial load on the

#### \* Corresponding Author:

Sinan Abdulkhaleq Yaseen

E-mail: [sinan.yaseen@su.edu.krd](mailto:sinan.yaseen@su.edu.krd)

#### Article History:

Received:19/12/2019

Accepted: 19/02/2020

Published: 08/09 /2020

STFC columns with laterally subjected cyclic load. From the analysis, a simplified lateral hysteretic load versus lateral deformation model. Fa-xing et al. studied composite frame consists of STFC circular column joined with steel- concrete beam under subjected to cyclic lateral loading (Fa-xing et al., 2018). The obtained outcomes from the modeling of FE were in shows very close agreement while comparing with experimental data in terms of modes of failure, load-displacement response curves, and skeleton curves.

The behavior investigation is the main objective of this work to see the behavior of STFC framed to steel sectioned beam and loaded to maximum load allowed by AISC steel manual (AISC, 2005), and subjected to an increasing lateral load. A FE modelling using ANSYS program (ANSYS, 2016) was developed to analyze the frame. The AISC design parameters, namely height-to-size L/D with size-to-thickness of the section skin D/t ratios of STFC, are investigated. The aim of the research is to study the effects of column height and skin thickness, based on those available in the AISC manual, on the load-deformation reaction of composite frames, including steel tubes filled with concrete STFC, loaded by maximum vertical load allowed by AISC manual

## 2. Composite Frames Used in the FE Analysis

Table (1) shows details of nine STFC connected to steel beam. The used material properties were the strength of concrete (28 MPa) and the yield strength of steel (290 MPa). Fig. (1) Shows views of the composite frame with a close view of the connection of beam with columns, and column with base plate connection. The beam has total span of (4775 mm) with standard section specification of (W12x106), (AISC, 2005).

Table (1) Details of the STFC Frame.

Frame	fc MPa	Fy MPa	Outer Dia.(mm)	Skin Thick. (mm)	D/t	Effective Height (mm)	L/D	Vertical load per (ASD) (No) kN
L10-t1	28	290	254	14.76	17.21	3048	12	1939
L10-t2	28	290	254	8.86	28.65	3048	12	1428
L10-t3	28	290	254	5.92	42.92	3048	12	1152
L15-t1	28	290	254	14.76	17.21	4572	18	1753
L15-t2	28	290	254	8.86	28.65	4572	18	1272
L15-t3	28	290	254	5.92	42.92	4572	18	1023
L20-t1	28	290	254	14.76	17.21	6096	24	1481
L20-t2	28	290	254	8.86	28.65	6096	24	1085
L20-t3	28	290	254	5.92	42.92	6096	24	863

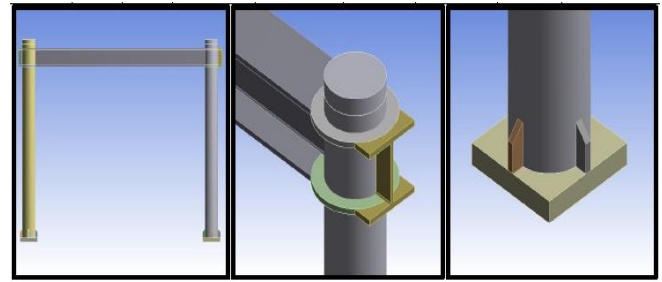


Figure 1: Typical composite frame.

## 3. Modelling

FE modelling using ANSYS was carried out. The element modeling of circular steel shell, stiffening ribs and steel beams were constructed according to solid 186 element. While solid 185 element was used for modeling A (50.0) mm thick steel base plate, which was added at the fixed support locations for the STFC in order to prevent any problems caused by stress concentration. This plate more range in stress distribution that applied on supports. Each finite element has eight nodes, the number of degree of freedom are three for three main directions in each node. To represent concrete material for in the FE simulation, solid 65 element was used. Like the previous element definition, each finite element has eight nodes, the number of degree of freedom are three for three main directions in each node. The mentioned elements have of plastic deformation, cracking, and crushing ability in three directions. The mesh sizes were changed to reach to the full fit one in terms of results stability and consuming elapsed time. The chosen meshes that used for composite simulated frames are shown in Fig. (2) (Yaseen, 2020). The friction coefficient between the interface of steel shell and core concrete was taken to be 0.35 (Lin-Hai, 2011). while the elastic modulus and Poisson's ratio for concrete material were 25.0 GPa and 0.2, respectively, for all studied models. The ANSYS program allow a bilinear or multi linear steel stress-strain curves, the modulus of elasticity and Poisson's ratio for elastic stage up to proportional limit were 210 GPa, and Poisson's ratio of 0.3.

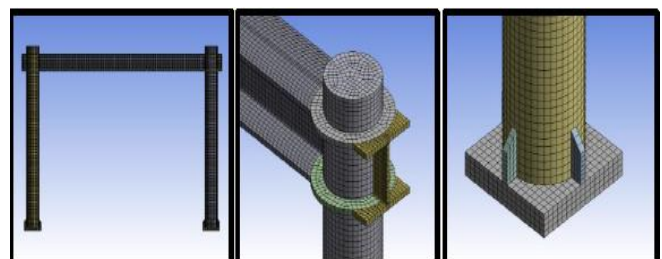


Figure 2: Mesh distribution for the composite frame.

### 3.1. Material Properties

The properties of the STFC frame material are defined as follows:

#### 3.1.1. Concrete

The construction of these types of element is obstacle to make a real represented member in behavior point of view, by having a quasi-brittle property and changing behavior by concrete in both compression and tension. Normal weight Concrete obeys atypical stress-strain relation curve (Bangash, 1989) when as the strength range defined to be 28 MPa as shown in Fig. (3). The load deformation response in compression for concrete from linearly elastic range up to 40% when exceed the stress of maximum limits. A gradual increase increment it seen in the merge of maximum limit point  $\sigma_{cu}$ , starting to descend into a softening region, and eventually crushing failure modes occurs when reaching the ultimate strain limits  $\epsilon_{cu}$ . The material load deflection response behave to be linear elastic to maximum limits in tensile strength in tension, occurring cracks start after that to decrease the carrying capacity gradually to zero (Bangash, 1989). However, using this ideal relation curve work as a negative slope portion was not preferred in defining finite element materials which lead to convergence problems.

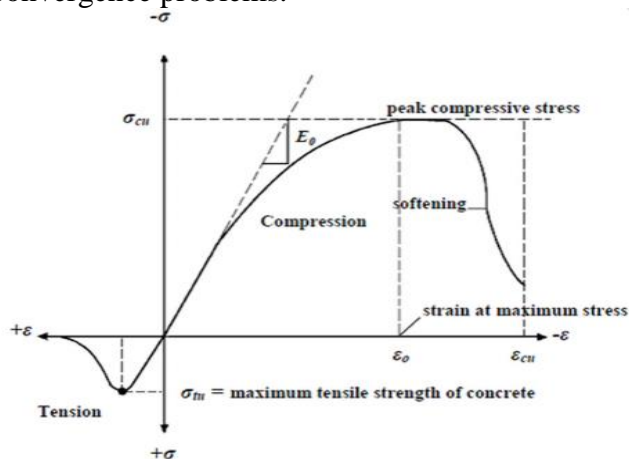


Figure 3: Typical Uniaxial Compressive and Tensile Stress-Strain Curve for Concrete (Bangash, 1989).

The uniaxial stress-strain relationship is required in defining concrete material in ANSYS program in compression. To consider a uniaxial compressive stress-strain in construction the concrete response curve, some numerical equations that used by (Desayi & Krishnan, 1964), Equations (1) and (2), were used that work with all strength range along with Equation (3) (Bangash, 1989).

$$f = \frac{E_c \epsilon}{1 + \left(\frac{\epsilon}{\epsilon_0}\right)^2} \tag{1}$$

$$\epsilon_0 = \frac{2f'_c}{E_c} \tag{2}$$

$$E_c = \frac{f}{\epsilon} \tag{3}$$

$f$  = Stress at any strain  $\epsilon$

$\epsilon$  = Strain at stress  $f$

$\epsilon_0$  = Strain at the ultimate compressive strength  $f'_c$

A compressive uniaxial stress-strain relationship is simplified and shown as in Fig. (4), which is for each STFC model to constructed well consist six points connected by straight lines. The linear stage was up (0.30 $f'_c$ ) of the curve that starts from at zero stress and strain to be point No.1engaging equation (3). While equation (1) employing modulus of elasticity, initial strain, and strains for stress evaluation in all points No. 2, 3, and 4, the initial strain  $\epsilon_0$  is calculated from Equation (2) by using concrete compressive strength and the modulus of elasticity. In the fifth point an assumption was made of perfectly plastic behavior at  $\epsilon_0$  and  $f'_c$  to be point 5.

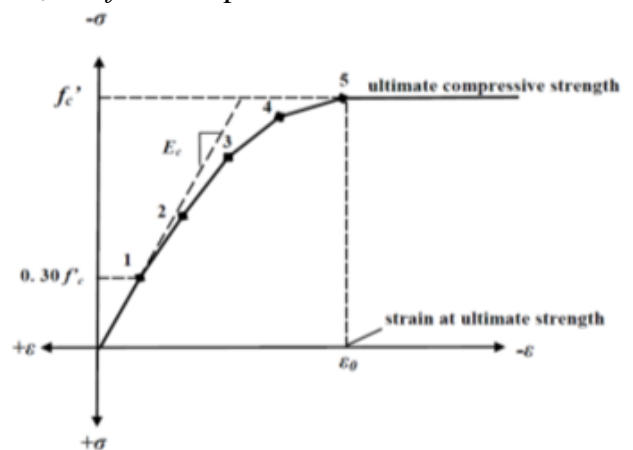


Figure 4: Simplified compressive uniaxial stress-strain curve for concrete (Desayi and Krishnan, 1964).

#### 3.1.2. Steel Tube Column and Base Plates

An actual stress strain response curve is the outcome from tensile tests, which used to be a tensile stress-strain curve in defining steel properties in the finite element model. However, to removing the negative slope portion of the curve from this stress-strain curve, the response was modified to gain the more convergence in finite element model, and a modification performed in zero slop part after yield to a mild positive slope.

### 3.2. Verification of the FE Model

The experimental data results used for comparison with the FE model as a validity verification. The element column beam connection STFC in composite frames tested by Lin-Hai Hana et al. are used in this paper to verify the proposed FE model using ANSYS program. For frame (CF-13) (Lin-Hai, 2011), with circular STFC columns, the basic information is;

1.45m was clear frame column height with 2.5m beam span. The used column tube size was 140mm in diameter and 2mm thickness. The beam's section dimensions are; 140mm depth, 65mm flange width, 3.44mm flange thickness, and 3.44 web thickness. The mechanical properties are presented in table (2) for the beam and STFC column element. The result data of verification analysis are given in table (3), Fig. (5) Shows the deflected shape of the frame under FE model analysis using ANSYS program. Figs (6) to (8) show the maximum principal stresses at the regions of frame connections.

The comparison shows that high accuracy has been achieved for the FE model using ANSYS program in predicting the load-displacement relationship of the composite frames.

**Table 2.** the material properties of the steel STFC frame [7].

Element	Yielding Strength $f_y$ (N/mm <sup>2</sup> )	Ultimate Strength $f_u$ (N/mm <sup>2</sup> )	Modulus of Elasticity $E_s$ (N/mm <sup>2</sup> )	Poisson's Ratio $\nu$
STFC Column	327.7	397.9	$2.063 \times 10^5$	0.266
Steel Beam	303.0	440.9	$2.061 \times 10^5$	0.262

**Table 3.** the verified theoretical and the experimental results.

Item	The experimental[7]	The theoretical FE model results	Theor./Exp. %
Axial Load of STFC Column (kN)(Constant)	410	410	100
Ultimate Lateral Load (kN)/Ultimate Frame Capacity)	55.25	55.6	101
Lateral Displacement of the frame at yield (mm)	12.5	12.46	101

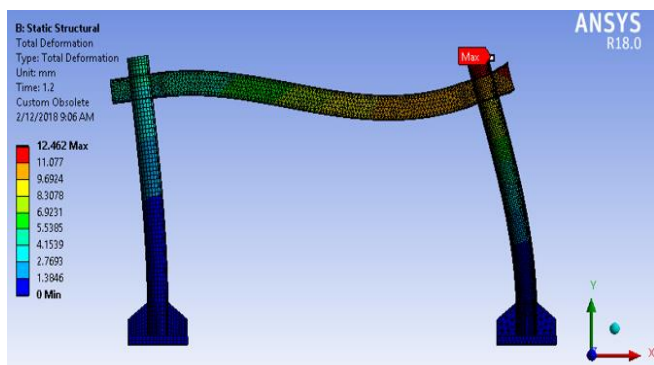


**Figure 5:** The deflected shape of the Lin-Hai Hana et al. frame under FE model analysis for verification using ANSYS program (Lin-Hai et al., 2008).

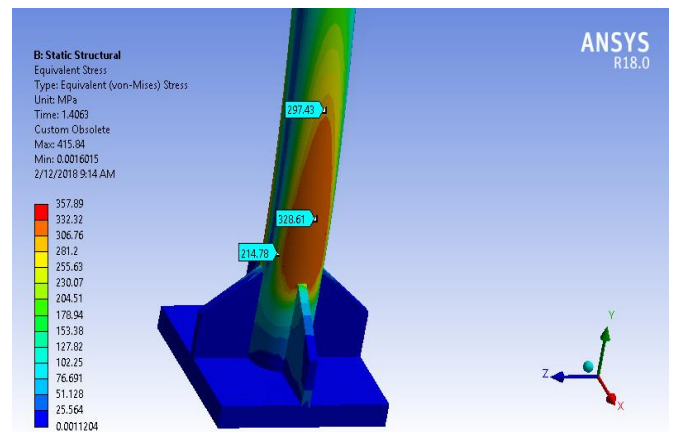


**Figure 6:** Maximum principal stresses at the region of the right column-base connection of Lin-Hai Hana et al. frame for verification purposes (Lin-Hai et al., 2008).

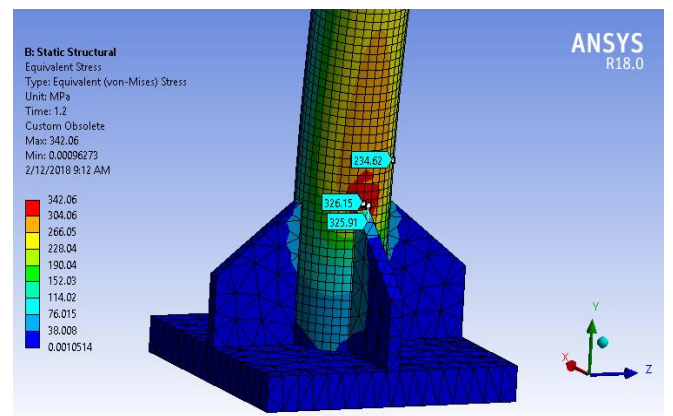


**Figure 7:** Maximum principal stresses at the region of the left column-base connection of Lin-Hai Hana et al. frame for verification purposes (Lin-Hai et al., 2008).

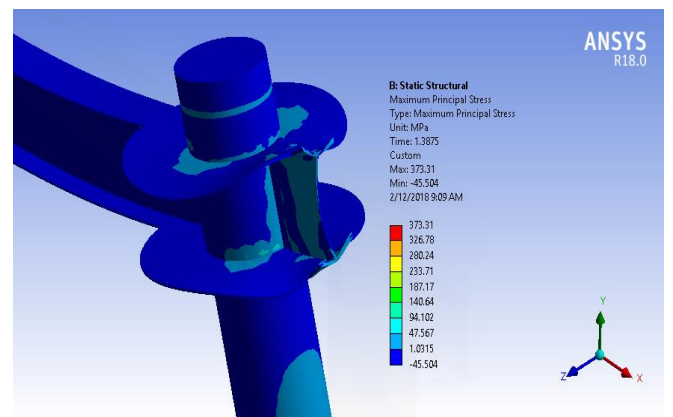


**Figure 8:** Maximum principal stresses at the region of the beam-column connection of Lin-Hai Hana et al. frame for verification purposes (Lin-Hai et al., 2008).

### 3.3. Analysis Type and Boundary Conditions

The static analysis type is utilized for the finite element model. In nonlinear analysis, the total load applied to a finite element model is divided into a series of load increments called load steps. At the completion of each incremental solution, the stiffness matrix of the model is adjusted to reflect nonlinear changes in structural stiffness before proceeding to the next load increment. The ANSYS program (ANSYS 18) (ANSYS, 2016) uses Newton-Raphson equilibrium iterations for updating the model stiffness. Newton-Raphson equilibrium iterations provide convergence at the end of each load increment within a tolerance limit.

## 4. Result and discussion

### 4.1. Failure Modes

Figs. (9) and (10) show failure modes and maximum stresses resulted from FE analysis. All the composite frames exhibited similar failure mode. Plastic hinges were formed at the top and the bottom of the STFC. No concrete core crush was observed. Thus, composite action was maintained throughout.

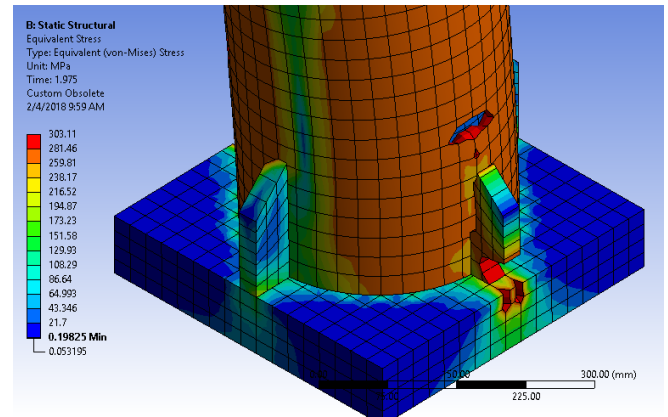
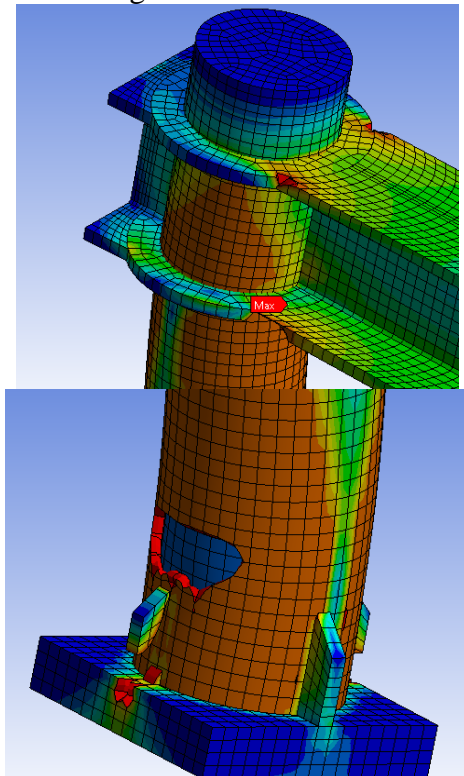


**Figure 9:** Failure mode and maximum stresses column-base connections.

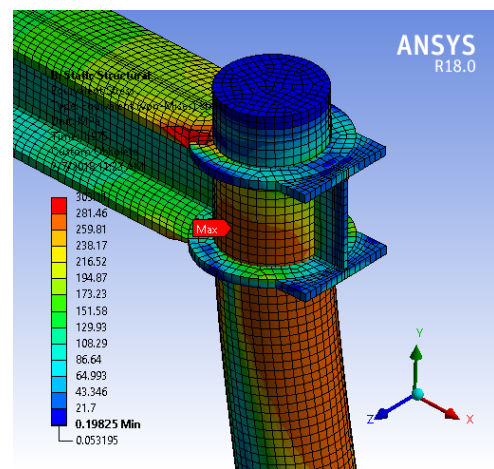
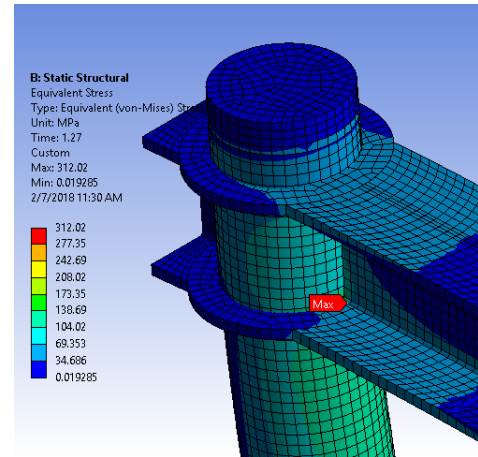


**Figure 10:** Maximum stresses at beam-column connection.

### 4.2. Maximum Stresses

Maximum stresses maps are shown in Figs. (9) and (10). Maximum stress occurred at the connection with the steel beam which was 312MPa. These figures show the stress distribution at the steel shell. The greater values are shown at the beam-column connection and at the top and bottom regions of the STFC. The maximum value 312 MPa ( $> 290$  MPa) indicates a plastic hinge formation at the connection of the steel beam and the top of the STFC, showing the

connection fixing ability that allow the hinge to occur close to the connection point.

### 4.3. Load Displacement Response

Figs. (11-13), show the lateral load – lateral displacement curves for STFC length, L = (3048 mm, 4572mm, and 6096mm), for steel shell thicknesses, t = (14.76 mm), (8.86 mm), and (5.92 mm), respectively. The load-strain curve for a composite frame at top connection is shown in Fig. (14).

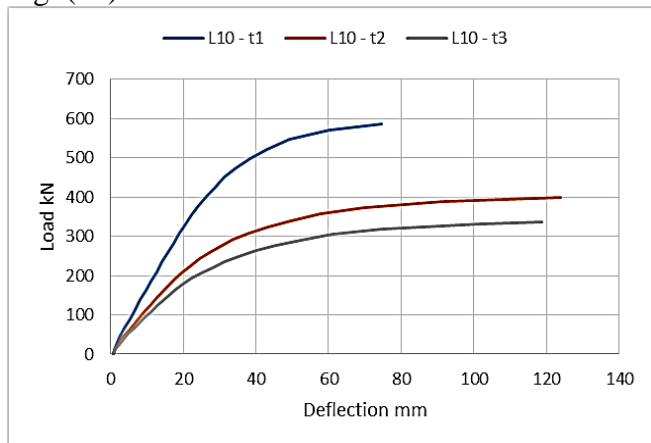


**Figure 11:** Lateral load – lateral displacement curves for STFC length, L = (3048 mm), for various steel shell thicknesses t = 14.76mm.

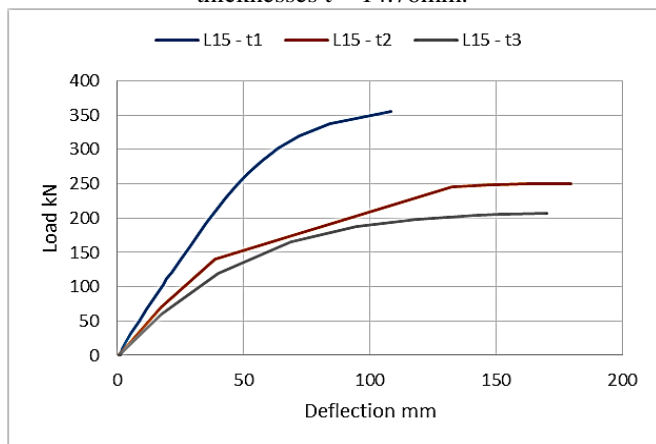


**Figure 12:** Lateral load – lateral displacement curves for STFC length, L = (4572 mm), for various steel shell thicknesses t = 8.86mm.

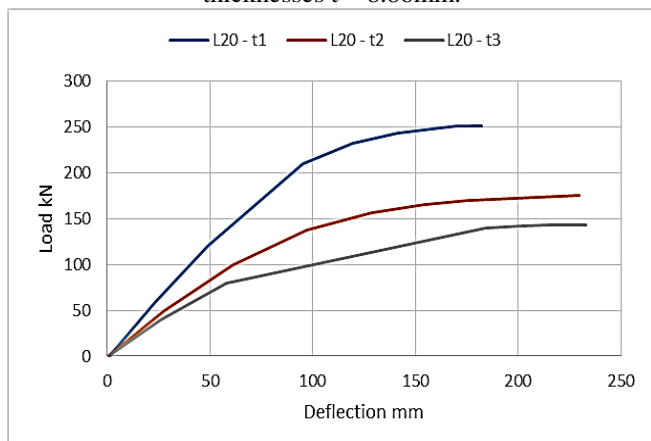


**Figure 13:** Lateral load – lateral displacement curves for STFC length, L = (6096 mm), for various steel shell thicknesses t = 5.92mm.

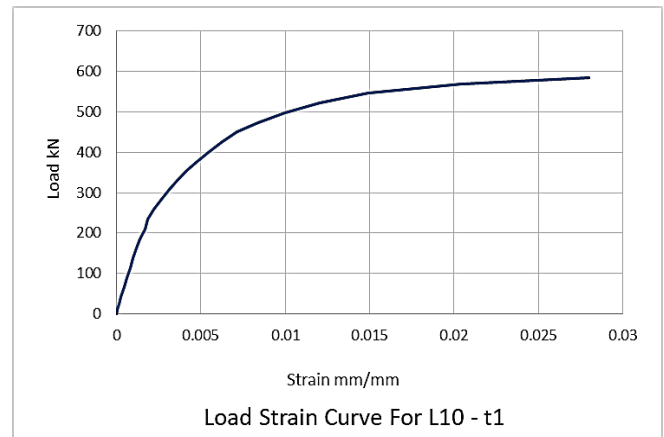


**Figure 14:** Load-strain curve for Frame L10-t1 at top connection.

From the figures it can be seen that STFC with steel shells of t = 14.76 mm shows the stronger and stiffer response over the other thicknesses which generally yielded close results to each other. At length L = 3048 mm, ratios of STFC of steel shell thickness t = 14.76 mm strength to those STFC of t = 8.86 mm. and of t = 5.92 mm. at ultimate stage were 402.6 kN /180.22 kN = 2.24, and 402.6 kN / 150.12 kN = 2.68.

Effect of column height can be also evaluated. It can be shown that STFC with steel shell of t = 14.76 mm. ratios of STFC of height L = 3048 mm. strength to those STFC of L = 4572 mm. and of L = 6096 mm. at ultimate stage were 402.6 kN /284.42 kN = 1.42, and 402.6 kN / 210.10 kN = 1.92.

Table (4) shows the lateral loads at yield and at failure, and the corresponding lateral displacements, for the studied AISC-STFC composite frames.

**Table (4)** Lateral loads at yield and at failure, and the corresponding lateral displacements, for the composite frames.

Frame	Hight (mm)	Skin thickness (mm)	$\Delta_y$ (mm)	$P_y$ (kN)	$\Delta_u$ (mm)	$P_u$ (kN)
L10 - t1	3048	14.76	9.66	162	26.1	402.6
L10 - t2	3048	8.86	9.5	94	19.88	180.22
L10 - t3	3048	5.92	9.4	80.5	16.1	150.12
L15 - t1	4572	14.76	19.4	125.8	53.4	284.42
L15 - t2	4572	8.86	13.5	79.4	35.8	139.5
L15 - t3	4572	5.92	11.8	65.4	36.34	120.25
L20 - t1	6096	14.76	40.5	100.45	95.01	210.1
L20 - t2	6096	8.86	29.4	52.95	61.15	100.95
L20 - t3	6096	5.92	25.9	40.18	57.93	80.45

#### 4.4. Lateral to Vertical Load Ratio

The composite frames of this study were loaded by the maximum value allowed by the AISC (AISC, 2005). Table (5) gives the percentage of lateral load (P) to the maximum allowed vertical load (No), at yield and at failure. The range of lateral load to maximum vertical load, at yield was (4.6 – 8.4%), and at failure was (9.2 – 20.8%). Greatest percentage of lateral loads are obtained for L =3048 mm. height and lower but similar percentages for L = 4572 mm. and L =6096 mm. height frames. The lower percentage in general may be due to the fact that the STFCs are loaded with max allowed load by the AISC.

**Table (5)** Percentages of lateral load (P) to maximum vertical load (No), at yield and at ultimate.

Frame	$P_y / N_o$ %	$P_u / N_o$ %
L10 - t1	8.4	20.8
L10 - t2	6.6	12.6
L10 - t3	7	13
L15 - t1	7.3	16.4
L15 - t2	6.2	11
L15 - t3	6.4	11.8
L20 - t1	6.8	14.2
L20 - t2	4.9	9.3
L20 - t3	4.7	9.3

#### 4.5. Displacement Ductility

Table (6) shows the displacement ductility ( $\Delta_u / \Delta_y$ ) ratios for the composite frames of this work. The range of ductility ratios is 1.71 to 3.06 with an average of 2.43 indicates good ductility of the composite frames (Lin-Hai, 2011). No indication is found on the effect of slenderness on the ductility. It should be reminded that the STFCs are loaded with maximum load allowed by AISC which affects the lateral load value and hence the lateral displacement at failure will be lower.

**Table (6)** Displacement ductility ( $\Delta_u / \Delta_y$ ) ratios for the composite frames.

Frame	$D_u / D_y$
L10 - t1	2.7
L10 - t2	2.09
L10 - t3	1.71
L15 - t1	2.75
L15 - t2	2.65
L15 - t3	3.08
L20 - t1	2.35
L20 - t2	2.08
L20 - t3	2.24

#### 5. Conclusions

The structural response of composite frames consisted of STFC columns connected to steel beam was investigated. The FE modeling was used to analyze the frames using ANSYS. The STFC columns were those listed in AISC steel manual. Lateral load was applied to failure. The following conclusions can be drawn:

- 1.All the composite frames exhibited similar failure mode. Plastic hinges were formed at the top and at the bottom of the STFC. No concrete core crush was observed. Thus, composite action was maintained throughout.
- 2.Maximum stress occurred at the connection with the steel beam was 312 MPa indicating a plastic hinge formation.
- 3.Load-displacement response shows significant stiffness and strength of AISC-STFC column of thickness  $t = 0.581$  in. (14.7 mm). This column with length  $L = 10$  ft. has a strength 2.24 times that of the column with  $t = 0.349$  in., and 2.68 times that of  $t = 0.233$  in.
- 4.Effect of column height was evaluated. For STFC with steel shells of  $t = 14.76$  mm., ratios of STFC of height  $L = 3048$  mm. strength to those STFC of  $L = 4572$  mm. and of  $L = 6096$  mm. at ultimate stage were 1.42 and 1.92, respectively.
- 5.The range of lateral load to maximum vertical load, at yield was (4.6 – 8.4%), and at failure was (9.2 – 20.8%). Greatest percentages of lateral loads are obtained for L =3048 mm. height.
- 6.The range of ductility ratios was 1.71 to 3.06 with an average of 2.43. Greater ductility ratio may be obtained should the vertical loads of the AISC STFC columns were reduced.

#### References

- AISC, (2005). American Institute of Steel Construction, Manual of Steel Construction, 13th Edition. Chicago.
- AHMED G.H. (2015). Mechanical Properties for Splices of Welded Reinforcing Steel Bars, ZANCO Journal of Pure and Applied Sciences, 27(6), 99-112.
- ANSYS, (2016). ANSYS User's Manual Revision 5.5. ANSYS, Inc., Canonsburg, Pennsylvania.
- BANGASH, M. Y. H. (1989). Concrete and Concrete Structures: Numerical Modeling and Applications. London: Elsevier Science Publishers Ltd.
- DESAYI, P. AND KRISHNAN, S., (1964). Equation for the Stress-Strain Curve of Concrete. Journal of the American Concrete Institute, 61(3), 345-350.

- FA-XING DING, GUO-AN YIN, LI-ZHONG JIANG, YU BAI (2018). Composite frame of circular STFC column to steel-concrete composite beam under lateral cyclic loading. *Thin-walled Structures*, (122), 137-146.
- HU H.T., HUANG C.S., WU M.H., WU Y.M. (2003). Nonlinear analysis of axially loaded concrete-filled tube columns with confinement effect. *Journal of Structural Engineering*, ASCE 2003;129(10), 1322-9.
- HAN L.H., YAO G.H., TAO Z. (2007). Performance of concrete-filled thin-walled steel tubes under pure torsion. *Thin-Walled Structures*, 45(1), 24-36.
- LIN-HAI HAN, WEN-DA WANG, XIAO-LING ZHAO (2008). Behavior of steel beam to concrete-filled SHS column frames: Finite element model and verifications, *Engineering Structures*, 30(6), 1647-1658.
- LIN-HAI HAN, WEN-DA WANG, ZHONG TAO (2011). Performance of circular STFC column to steel beam frames under lateral cyclic loading. *Journal of Constructional Steel Research*, 67(5), 876-890
- SCHNEIDER S.P. (1998). Axially concrete-filled steel tubes. *Journal of Structural Engineering*, ASCE 1998;124(10), 1125.
- SHAMS M, SAADEGHVAZIRI MA (1997). State of the art of concrete-filled steel tubular columns. *ACI Structural Journal*, 94(5), 558-571.
- YASEEN, S.A. (2020). Flexural Behavior of Self Compacting Concrete T-Beams Reinforced With ARFP. *ZANCO Journal of Pure and Applied Sciences*, 32(3).
- ZHAO X.L., GRZEBIETA R.H. (1999). Void-Filled SHS beams subjected to large deformation cyclic bending. *Journal of Structural Engineering*, ASCE, 125(9), 1020.